The Infrared Dichroism of Transmembrane Helical Polypeptides

P. H. Axelsen,* B. K. Kaufman,* R. N. McElhaney,‡ and R. N. A. H. Lewis‡
*Department of Pharmacology, University of Pennsylvania, Philadelphia, Pennsylvania 19104-6084 USA; and ‡Department of Biochemistry, University of Alberta, Edmonton, Alberta, Canada T6G 2H7

ABSTRACT Polarized attenuated total internal reflectance techniques were applied to study the infrared dichroism of the amide I transition moment in two membrane-bound peptides that are known to form oriented transmembrane helices: gramicidin A in a supported phospholipid monolayer and Ac-Lys_2-Leu_{24}-Lys_2-amide (L_{24}) in oriented multibilayers. These studies were performed to test the ability of these techniques to determine the orientation of these peptides, to verify the value of optical parameters used to calculate electric field strengths, to examine the common assumptions regarding the amide I transition moment orientation, and to ascertain the effect of surface imperfections on molecular disorder. The two peptides exhibit marked differences in the shape and frequency of their amide I absorption bands. Yet both peptides are highly ordered and oriented with their helical axes perpendicular to the membrane surface. In the α-helix formed by L_{24}, there is evidence for a mode with type E_1 symmetry contributing to amide I, and the amide I transition moment must be more closely aligned with the peptide C═O (<34°) than earlier studies have suggested. These results indicate that long-standing assumptions about the orientation of amide I in a peptide require some revision, but that in general, infrared spectroscopy yields reliable information about the orientation of membrane-bound helical peptides.

INTRODUCTION

Fourier-transform infrared (FTIR) spectroscopy is being used with increasing frequency to identify polypeptide helices in lipid membranes and to determine their orientation. The focus of these studies is usually the amide I region of the mid-IR spectrum (1600–1700 cm^{-1}) because the location, shape, and intensity of amide I absorptions are a rich potential source of information about peptide conformation (Susi et al., 1967; Braiman and Rothschild, 1988; Mantsch and Surewicz, 1991; Arrondo et al., 1993). The orientational order of helical secondary structures may be estimated from measurements of amide I dichroism using transmission techniques (e.g. Rothschild and Clark, 1979), although polarized attenuated total internal reflectance (PATIR) offers particular advantages for this purpose (Harrick, 1967; Axelsen et al., 1995) and is becoming an increasingly popular approach.

Theory pertaining to infrared dichroism and internal reflectance is well developed (Fraser and Price, 1952; Fraser 1953, 1956, 1958; Harrick 1967; Hansen 1968, 1972, 1973), and an order parameter for the amide I vibrational transition moment may be derived directly from dichroism measurements. However, most studies of membrane-bound helices seek a "molecular order parameter," which describes the overall orientation of a helix. This requires information about the orientation of the amide I transition moment with respect to the peptide backbone. The amide I band has complex origins arising from displacements within the H—N—C═O group, and it is strongly influenced both by hydrogen-bonding relationships and by dipole coupling with neighboring groups (Krimm and Bandekar, 1986; Krimm and Reisdorf, 1994). As such, the orientation of the amide I transition moment within the peptide group is difficult to predict and is likely to vary, depending on its conformational circumstances.

Virtually all PATIR-FTIR studies to date ultimately rely on the early transmission IR studies of α-helical polymeric aspartate or glutamate derivatives by Miyazawa and Blout (1961), Tsuboi (1962), or Bradbury et al. (1962) for information about the orientation of the amide I transition moment. For reasons discussed below, these results may not be fully applicable to membrane-bound peptides, and they do not apply, obviously, to peptides that are not α-helical. Therefore, we have undertaken a study of two membrane-bound peptides whose helical structure and orientation within a membrane are already known with a high level of confidence. By comparing the order parameters derived from the known structures of these peptides to those derived by our spectroscopic studies, we aim to test the reliability of assumptions commonly made in PATIR-FTIR studies.

The first peptide, gramicidin A, is a linear pentadecapeptide originally isolated from *Bacillus brevis*, which forms ion-selective membrane channels. It comprises alternating L- and D-amino acids:

HCO-L-Val-Gly-L-Ala-D-Leu-L-Ala-D-Val-L-
Val-D-Val-L-Trp-D-Leu-L-Trp-D-Leu-L-Trp-
D-Leu-L-Trp-$NHCH_2CH_2OH$.

Membrane-bound gramicidin is known to adopt two different conformations: a bilayer-spanning dimeric helix defined by x-ray crystallography (Wallace, 1992) and a homodimer of monolayer-spanning $\beta^{6.3}$ helical monomers defined by

Received for publication 11 May 1995 and in final form 4 September 1995.
Address reprint requests to Paul H. Axelsen, Department of Pharmacology, University of Pennsylvania, 3620 Hamilton Walk, Philadelphia, PA 19104-6084. Tel.: 215-898-9238; Fax: 215-573-2236; E-mail: axe@pharm.med.upenn.edu.

0006-3495/95/12/2770/12 $2.00

2D-NMR (Arseniev et al., 1985; Prosser et al., 1991; Ketchem et al., 1993). In the studies below, gramicidin is confined to a lipid monolayer, and thus we assume that it represents the latter structure.

The second peptide, acetyl-Lys_2-Leu_{24}-Lys_2-amide (L_{24}), was designed to be a model of the transmembrane α-helical segment of proteins such as glycophorin. This peptide consists of a single hydrophobic polyleucine segment capped at both N- and C-termini by two positively charged lysine residues. L_{24} and several structurally related peptides are known to form α-helices that span the hydrophobic core of a lipid bilayer and position the lysine termini at the membrane surface (Davis et al., 1983; Bolen and Holloway, 1990; Zhang et al. 1992a,b, 1995a,b,c). Both x-ray diffraction (Hulschilt et al., 1989) and earlier PATIR-FTIR studies (Zhang et al., 1995b) have strongly suggested that peptides of this type preferentially orient perpendicular to the membrane surface. However, the uncertain macroscopic orientation of the host membranes in these studies precluded a definitive study of peptide orientation.

We have also examined *N*-acetyl-tryptophan-amide (NATA) in order to evaluate the reliability of our spectroscopic analyses under circumstances in which absorption moments are likely to be unoriented (isotropic). Our results strongly support the validity of PATIR-FTIR techniques for the determination of amide I transition order and orientation. However, they also illustrate the weakness of long-standing assumptions used to transform order parameters for the amide I transition moment into molecular order parameters and the need to revise conclusions that rely on these assumptions.

MATERIALS AND METHODS

Lipids were purchased from Avanti Polar Lipids (Alabaster, AL). D_2O was obtained from Cambridge Isotope Laboratories (Woburn, MA). Gramicidin A was obtained from Fluka (Ronkonkoma, NY). L_{24} was a gift from Dr. Robert S. Hodges, Department of Biochemistry and MRC Group in Protein Structure and Function, University of Alberta, Edmonton, Canada. L_{24} was synthesized, purified, and prepared for study as described previously (Zhang et al., 1995b). NATA was obtained from Sigma (St. Louis, MO). All water originated from a reverse osmosis source and was glass distilled after passing through deionizing and organic removal filter systems (Mar-Cor Services, Harleysville, PA).

The instrument used in this work is described in detail elsewhere (Axelsen et al., 1995). Briefly, the beam from a Bio-Rad Digilab FTS-60A spectrometer is diverted outside the spectrometer to one of two 45° facets on the top of a 9 × 9 × 36 mm germanium crystal (Harrick Scientific, Ossining, NY). The beam emerging from the other 45° facet is directed to a narrow-band MCT detector (see Fig. 1). Before each experiment, the germanium crystal is sonicated first in detergent, then in 100% methanol followed by water, plasma-cleaned for 10 min at 100W (Harrick Scientific), and treated with 0.1% octadecyldimethyl[3-(trimethoxysilyl)propyl]ammonium chloride (50% solution in MeOH from Pfaltz and Bauer, Waterbury CT) in 95% ethanol and 5% water to produce a hydrophobic surface. The surface of these crystals was studied by atomic force microscopy (AFM) using a Dimension 3000 instrument from Digital Instruments (Santa Barbara, CA). Optical facets of the same germanium crystals used for spectroscopic studies were scanned in air, with and without prior silanization.

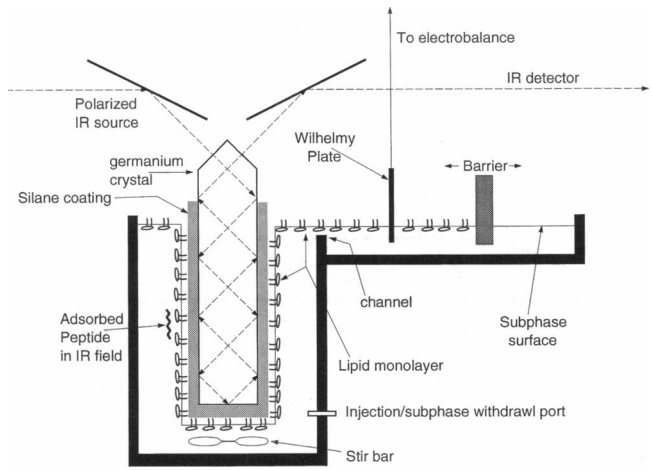

FIGURE 1 Schematic of the trough configuration. The apparatus is more fully described in Axelsen et al. (1995). The crystal remains stationary as the trough is raised to immerse the crystal into the subphase and apply the monolayer as shown. Monolayer surface pressure is measured by the Wilhelmy method and regulated by adjustment of the barrier position. Surface pressure is held constant during application of the monolayer to the crystal surface by a computer-controlled feedback loop involving the electrobalance and the barrier. The beam undergoes nine internal reflections within the crystal, of which seven interact with the applied monolayer.

For the gramicidin studies, a solution of gramicidin and 1,2-dimyristoyl-*sn*-glycero-3-phosphocholine (DMPC) at a 1:8 mol ratio in 90% hexane/10% ethanol was evaporated onto the surface of a D_2O-based buffer, at pH 7.0, containing 30 mM MOPS and 2 mM EDTA. The resulting monolayer was applied to the crystal surface at constant pressure using the Langmuir-Blodgett technique, as indicated in Fig. 1. For L_{24}, oriented multibilayers were produced by preparing a solution of acyl-deuterated 1,2-dipalmitoyl-*sn*-glycero-3-phosphocholine (DPPC) in methanol at a 1:10 mol ratio, applying it to the bottom end of an unsilanized crystal, and allowing it to evaporate. All experiments were performed at room temperature (21°C).

All spectra were derived from 1024 single-beam scans recorded at 2 cm^{-1} resolution, using triangular apodization, and one level of zero-filling. No smoothing or deconvolution was performed. Baseline correction, when done, was single point and level. Dichroic ratio determination was carried out by interactive subtraction of parallel and perpendicular absorbance spectra (see example below). Order parameters, S, as a function of the dichroic ratio, R_z, are given by:

$$S(R_Z) = \frac{E_X^2 - R_Z E_Y^2 + E_Z^2}{E_X^2 - E_Y^2 R_Z - 2E_Z^2}$$

where the dichroic ratio, R_z, is the ratio of parallel ($A_{\parallel}$) and perpendicular ($A_{\perp}$) absorption coefficients (Harrick, 1967; Fringeli and Gunthard, 1981). E_X^2, E_Y^2, and E_Z^2 represent the electric field amplitudes along the x, y, and z axes (defined in Fig. 2) and are given by

$$E_X^2 = \frac{4\cos^2\phi(\sin^2\phi - n_{31}^2)}{(1 - n_{31}^2)[(1 + n_{31}^2)\sin^2\phi - n_{31}^2]}$$

$$E_Y^2 = \frac{4\cos^2\phi}{(1 - n_{31}^2)}$$

and

$$E_Z^2 = \frac{4\cos^2\phi\, n_{32}^4 \sin^2\phi}{(1 - n_{31}^2)[(1 + n_{31}^2)\sin^2\phi - n_{31}^2]}.$$

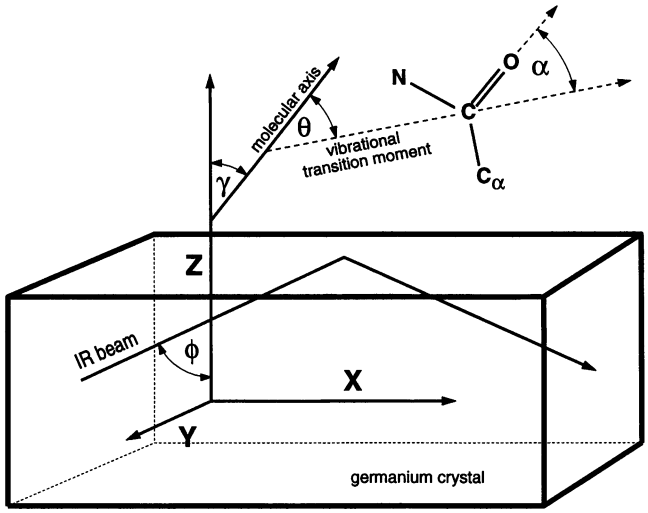

FIGURE 2 Coordinate and angle conventions used in this work. The XY plane is parallel to the germanium crystal surface, and the XZ plane is parallel to the plane of incidence. ϕ is the angle of incidence. γ is the angle formed by any conveniently defined molecular axis and the Z director; the equations given in the Methods section require that this axis be isotropically distributed in the XY plane. θ is the angle between the vibrational transition moment and the molecular axis, and as with γ, the equations given in Methods require that the transition moment be isotropically distributed in the plane perpendicular to the molecular axis. α is the angle between the transition moment and the peptide carbonyl bond and is determined assuming that the atoms shown are co-planar. The angle α is not to be confused with the subscript denoting the α carbon in an amino acid.

where n_1, n_2, and n_3 are the refractive indices of germanium, a thin film on the germanium surface, and the buffer, respectively; $n_{31} = n_3/n_1$ and $n_{32} = n_3/n_2$; and ϕ is the angle of incidence between the beam and a normal to the crystal surface. These equations pertain specifically to the field amplitude at the crystal surface. We assume that absorption of light within the thin layer is negligible (at the frequency of interest) and that the electric field strength is constant across its thickness. In addition, specific assumptions are made about angular distributions, as noted in the caption to Fig. 2.

$S_I(R_z)$ and $S_{II}(R_z)$ refer to the amide I and amide II transition, respectively. In this convention, $S = 1.0$ for a maximally ordered system aligned with the z axis, and $S = -0.5$ for a maximally ordered system aligned perpendicular to the z axis. For an isotropic (completely disordered) system, $S = 0.0$ and $R_z = R_{ISO} = (E_X^2 + E_Z^2)/E_Y^2$.

For anisotropic systems, we may write

$$S(R_Z) = \langle P_2(\cos\theta)\rangle\langle P_2(\cos\gamma)\rangle\langle P_2(\cos\xi)\rangle$$

where θ and γ describe angular relationships between the transition moment and the z axis and are defined explicitly in Fig. 2 for the case of a polypeptide. The angle ξ represents a measure of surface flatness and is 0° for a perfectly flat surface (see AFM results below for definition). P_2 is the second order Legendre polynomial, defined as $P_2(x) = (3x^2 - 1)/2$. For angles such as θ and γ, it is possible (but unlikely) that $\langle P_2(\cos x)\rangle = P_2(\cos\langle x\rangle)$. Nevertheless, it is common practice to employ this relationship and associate $\langle P_2(\cos x)\rangle$ with a single value of x that it not necessarily equal to $\langle x\rangle$ (see discussion of $\langle P_2\rangle$ in Appendix). For situations in which γ and ξ cannot be examined separately, the symbol γ_ξ is used to represent the angle that satisfies $P_2(\cos\gamma_\xi) = \langle P_2(\cos\gamma)\rangle\langle P_2(\cos\xi)\rangle$. Depending on the circumstances, either $P_2(\cos\gamma_\xi)$ or $\langle P_2(\cos\gamma)\rangle$ represents the "molecular order parameter."

For model peptides oriented parallel to the z axis, any given value for the angle between the transition moment and the C=O bond, α, yields a value θ_i for each of n pairs of C→O and N→C bond vectors. Using primes (′) to indicate values derived from molecular models, and given that $\gamma = \xi = 0°$ for such models, the relationship between model-derived and experimentally derived order parameters is given by:

$$S_I'(\alpha) = S_I'(\theta) = \langle P_2(\cos\theta)\rangle$$

$$= \frac{\left[\frac{3}{n}\Sigma(\cos^2\theta_i')\right] - 1}{2} = \frac{S_I(R_Z)}{P_2(\cos\gamma_\xi)}.$$

The analysis of lipid acyl chain order differs from that of amide I order because γ describes only a segment of the acyl chain. The vibrational transition moment orientation is defined as the bisector of the H—C—H angle, and the segmental orientation is mutually perpendicular to the two C→H bond vectors. Therefore, $\theta = 90°$, $P_2(\theta) = -1/2$, and relationships involving the lipid acyl chain order parameter, S_L, are given by

$$S_L'(\gamma) = \langle P_2(\cos\gamma)\rangle = \frac{\left[\frac{3}{n}\Sigma(\cos^2\gamma_i')\right] - 1}{2} = \frac{-2\,S_L(R_Z)}{\langle P_2(\cos\xi)\rangle}.$$

RESULTS

NATA

Measurements of R_z for NATA were made in order to test some of the major assumptions made in the calculation of electric field amplitudes on the crystal surface. We compared these measurements with a calculated value for R_{ISO}, assuming that the amide I transition moment of NATA is oriented isotropically with respect to the surface of a silanized germanium crystal. As seen in the equations above, R_{ISO} is a function of three refractive indices and ϕ.

Spectra were collected with the crystal immersed in a 50 mM solution of NATA in D_2O, using a sample of pure D_2O for background. This yielded absorbances in the range of $A_\parallel \approx 0.6$ and $A_\perp \approx 0.4$ at 1638 cm^{-1}, and dichroic ratios ranging from 1.58–1.67 (Fig. 3, *a* and *b*). Solutions of more soluble (zwitterionic) forms of tryptophan and phenylalanine as well as various other compounds at this concentration yielded no detectable absorbance, indicating that the signal obtained using NATA arises solely from material adsorbed to the hydrophobic crystal surface. For $n_1 = 4.00$, $n_2 = 1.40$, $n_3 = 1.32$ (Frey and Tamm, 1991), and $\phi = 45°$, the equations above indicate that an isotropically distributed sample should exhibit a dichroic ratio of 1.77 in D_2O at $\nu \approx$ 1650 cm^{-1}. This is outside the range of our experimental values (1.58–1.67), so we have examined five possible contributions to the discrepancy.

First, the RMS noise level for both polarization measurements is ~0.03 mA, and the error being considered corresponds to 8.5% of a 0.6 mA measurement, or 0.05 mA. Thus, the magnitude of the discrepancy is comparable to the noise, although it is sufficiently large to be demonstrable above the noise. This is seen by visual inspection in a plot of $(A_\parallel - 1.77 \cdot A_\perp)$ which clearly demonstrates residual dichroism (Fig. 3 *c*) and indicates that the measured dichroic ratio is less than 1.77.

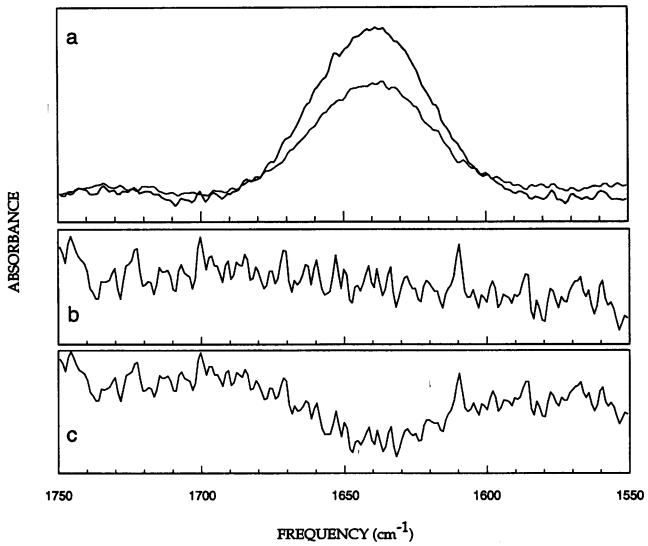

FIGURE 3 (*a*) Parallel (*thick line*) and perpendicularly polarized (*thin line*) absorption spectra ($A_{\parallel}$ and $A_{\perp}$, respectively) for *N*-acetyl-tryptophanamide adsorbed to a silanized germanium crystal surface. The spectra have not been smoothed, deconvolved, or subjected to baseline correction. (*b*) A plot of $[A_{\parallel} - 1.58 \cdot A_{\perp}]$ on an expanded ordinate scale. (*c*) A plot of $[A_{\parallel} - 1.77 \cdot A_{\perp}]$ on an expanded ordinate scale.

Second, polarizer "leakage" will contribute to error. In the analysis of Myers and Cooper (1994), this error is related to the leakage fraction, defined as the ratio of the light intensities transmitted perpendicular and parallel to the polarizer axis. For a given leakage fraction, the error magnitude will be ~1% of the value of R_z per 0.01 unit of leakage fraction, and the observed dichroism will be lower than the true dichroism. On the basis of our experience with crossed polarizers (Axelsen et al., 1995), we believe that the overall leakage fraction for our instrument is ≤2%. Therefore, this error will account for some, but not all, of the discrepancy (all values for R_z below are reported uncorrected, but are multiplied by 1.02 when used to calculate order parameters).

Third, our assumptions regarding the indices of refraction for the silane monolayer and D_2O may not be accurate. The indices most commonly used for the acyl chains of the silane and of lipids are based on the index for aliphatic hydrocarbons, and they do not account for effects such as optical anisotropy, which may arise because of the presence of nonhydrocarbon lipid head groups, the oxide layer on the germanium crystal, or the silane polymer. It is common to use $n_2 = 1.4$ in the vicinity of 1650 cm^{-1} and $n_2 = 1.5$ in the vicinity of 2900 cm^{-1} (Fringeli and Gunthard, 1981; Maoz and Sagiv, 1984; Frey and Tamm, 1991).

For D_2O, the most reliable index is apparently derived by manual extraction of the data from Fig. 2 of Sethna et al. (1978) and is between 1.31–1.33 over the frequency range 1630–1650 cm^{-1}. In Fig. 4 we illustrate the effect of this uncertainty in n_3 on n_2 and R_{ISO}. It is evident that values for n_2 must assume values of 1.46–1.48 in order to reconcile our measured value for R_z and our calculated value for R_{ISO}. These values for n_2 are plausible and sufficiently different from $n_2 = 1.40$ (which yields $R_{ISO} = 1.77$) to show that our uncertainty in the value of n_3 is not sufficient to account for the difference between R_z and R_{ISO}.

Fourth, we have assumed the angle of incidence to be 45°. Although this was verified in earlier work (Axelsen et al, 1995), the spectrometer beam is ~4 cm in diameter

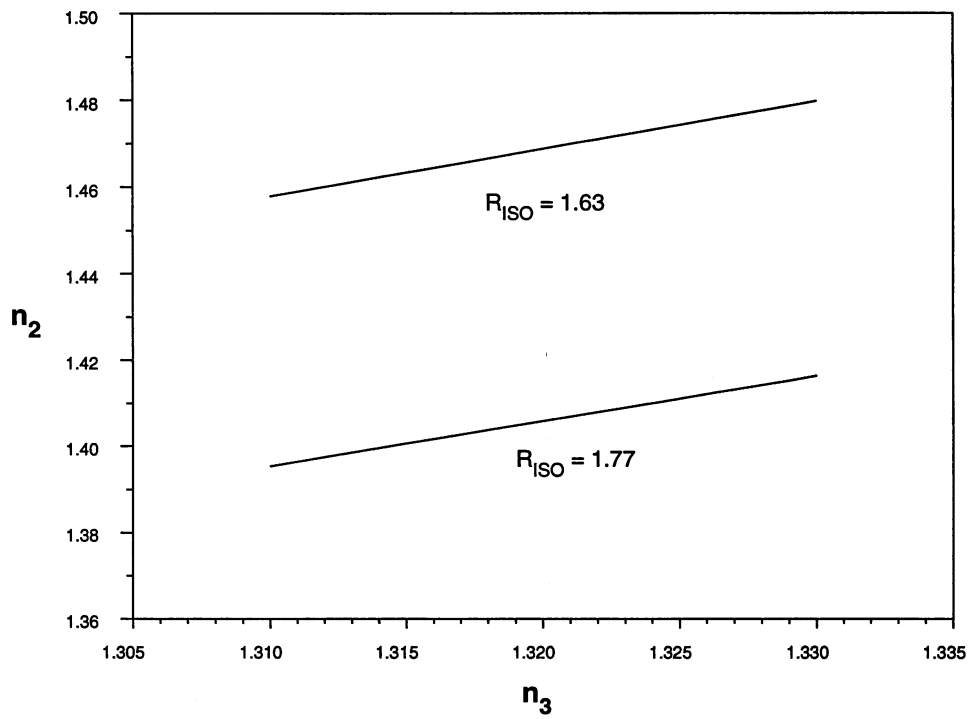

FIGURE 4 Relationships between R_{ISO}, n_2, and n_3 assuming that $n_1 = 4.00$ and $\phi = 45°$. It is apparent that uncertainty in the value of n_3 over the range 1.31–1.33 is not sufficient to account for the difference in R_{ISO} apart from a difference in n_2.

and focused on a 45° facet of the crystal using an off-axis parabolic mirror with a focal length of 5.72 in. Thus, portions of the the beam strike the crystal surface at 90 ± 8° and are refracted to 90 ± 2° upon entering the crystal. Our analysis of this divergence using the equations above indicates that its magnitude is likely to be negligible.

Finally, the sample we have studied may not be perfectly isotropic. An ideal test sample is difficult to devise, insofar as surface forces with the potential to orient the sample will always be present (see Discussion below). Assuming that the true isotropic ratio is indeed 1.77, a measured value of 1.63 corresponds to $S(R_z) = -0.06$. It seems entirely plausible that the system has this level of anisotropy.

In summary, we conclude that noise, assumptions regarding the effective value of n_3, and beam divergence contribute a relatively small amount of error to these measurements in comparison with our uncertainty in the value of n_2. Error due to imperfect polarization will contribute to an underestimation of R_{ISO}, but this error is both relatively small and correctable. The sample of NATA that we have studied may not be perfectly isotropic on the crystal surface, but it is sufficiently close to indicate that $n_2 \leq 1.48$. Correcting for a 2% polarizer leakage fraction reduces this upper limit to only ≤ 1.47. Our data do not establish a specific lower limit for n_2, but it is safe to assume that $n_2 \geq n_3$. This implicitly recognizes that electric fields in the vicinity of NATA may be governed more so by n_3, which in the limiting case of $n_2 = n_3$ is equivalent to neglecting the thin layer index and applying equations for a simple two-component interface. If $n_2 = n_3$, then $R_{ISO} = 2.00$ and $S(R_z) = -0.13$ for NATA.

Our data do not help identify errors that may compensate for each other. Nonetheless, they are an important test of our assumptions and of the performance of this instrument. Considering uncertainty due to noise, we believe that 1.4–1.5 is a reasonable working confidence interval for n_2 in this frequency range, and precision beyond two significant digits seems to be unwarranted at this point.

Germanium crystal surface

As received from our supplier, the germanium crystals used in this work have been mechanically polished with 0.3 μm alumina. It is our practice to hand-polish the crystal after each use with 0.1 μm alumina and a rare earth suspension in order to remove the old silane layer before resilanization. This cannot be expected to yield a surface that is flat on the order of molecular dimensions, and we must expect that surface imperfections will limit the maximum order that we can observe in a sample.

We examined both an unsilanized crystal and a silanized crystal with an AFM to characterize the surface of these crystals. The data obtained consisted of x and y positional information, and the z height for an array of 512 × 512 data points over 2 × 2 μm regions of the crystal. This provides a nominal resolution of 3.9 nm. If we estimate the area of a lipid molecule to be 0.6 nm^2, this suggests that each data point corresponds to ~25 lipid molecules. These data were analyzed in two ways. First, we calculated a value for $\langle P_2(\cos \xi) \rangle$ by determining the vectors normal to the triangular planes defined by every possible combination of three adjacent points, and the angle ξ between each vector and the z axis. Second, we calculated a local surface "curvature" by determining the radius of a sphere that is tangent to the midpoints in each pair of adjacent triangular planes.

These analyses yield values for $\langle P_2(\cos \xi) \rangle$ of 0.65 and 0.82 for the untreated and the silanized crystal, respectively. The most probable curvature was 20 nm for the untreated crystal surface and 50 nm for the silanized surface. The distribution of curvature values was distinctly skewed toward higher radii for the silanized crystal compared with the unsilanized crystal (Fig. 5). These results suggest that the acyl-silane chains effectively reduce surface imperfections and may explain our earlier report that the acyl chain order of a lipid monolayer tended to be higher than the acyl chains of the silanizing agent (Axelsen et al., 1995). In addition, the lipid monolayer may resist the formation of highly curved surfaces. In this case, $\langle P_2(\cos \xi) \rangle$ for the lipid surface (in contrast to the acyl-silane surface) may be >0.82. In lieu of comparable data for fully hydrated monolayers on germanium crystals, these studies provide a lower limit for surface order that is useful in the analyses below.

DMPC in gramicidin/DMPC

The structure of gramicidin in lipid membranes has been studied by NMR spectroscopy (Arseniev et al., 1985; Prosser et al., 1991; Ketchem et al., 1993), x-ray crystallography (Wallace, 1992), and molecular dynamics simulation (Roux and Karplus, 1994). The information provided

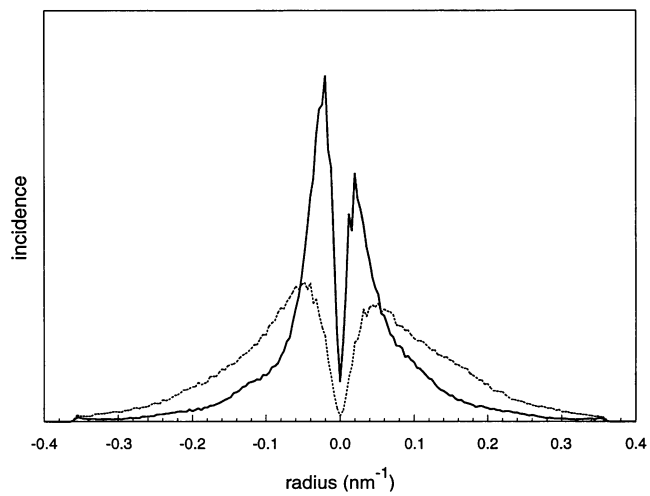

FIGURE 5 Germanium surface flattening due to silanization. The data from a 512 × 512 raster AFM scan are presented as a histogram of reciprocal values for the radius of a sphere, which is tangent to each pair of adjacent points. (——) represents an unsilanized crystal; (- - - -) is a silanized crystal.

by these studies permits direct comparison of experimentally determined and structure-derived order parameters with those derived from PATIR-FTIR measurements.

Lipid order parameters are derivable from the simulation structure (provided to the authors by B. Roux, University of Montreal, Montreal, Quebec) in which gramicidin assumes a $\beta^{6.3}$ conformation in a 1:8 mol ratio with a DMPC bilayer. We assume that the orientation of the symmetric stretching mode for lipid CH_2 groups at 2850 cm^{-1} is the bisector of each H—C—H angle and that the molecular axis at that point is perpendicular to the bisector (i.e., $\theta = 90°$). For the 12 CH_2 groups in each acyl chain and the four CH_2 groups of the polar headgroup, we calculate $\langle\cos^2\gamma\rangle$ for the 16 DMPC molecules in this simulation and obtain S_L (γ') = 0.61 using the equation given above. This value seems to agree with NMR-derived segmental order parameters for DMPC reported by Moser et al. (1989) and the report by Rice and Oldfield (1979) that this order is approximately the same when gramicidin and DMPC are present in a 1:8 ratio.

Experimentally, we applied gramicidin and DMPC in a 1:8 mol ratio as a monolayer to the germanium crystal surface, and we measured the dichroic ratio for the symmetric CH_2 stretching band at 2849.2 cm^{-1} to be 1.12 ± 0.05. For $n_2 = 1.45$, $n_3 = 1.225$, $\theta = 90°$, and $\langle P_2(\cos\xi)\rangle = 0.82$, this yields $-2\ S_L(R_z)/\langle P_2(\cos\ \xi)\rangle = 0.60$. This value, and S_L (γ') from the aforementioned experimental and simulation results, are in excellent quantitative agreement.

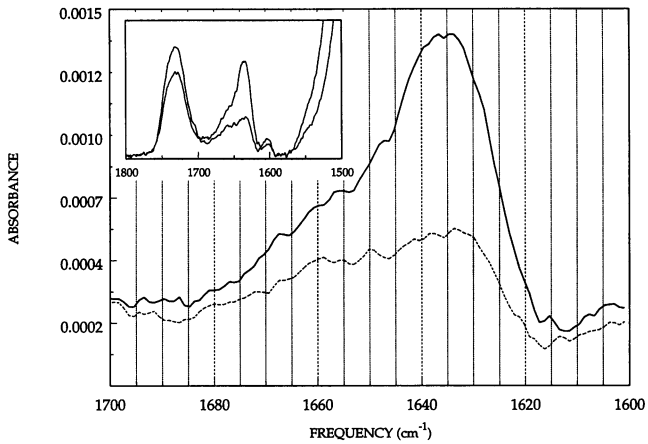

FIGURE 6 Parallel (*thick line*) and perpendicularly polarized (*thin line*) absorption spectra for a monolayer of gramicidin in DMPC. Inset: adjoining spectral regions showing baseline correction point (1800 cm^{-1}) and absorption due to lipid ester carbonyl stretching (1740 cm^{-1}). The spectra go off scale approaching 1500 cm^{-1} because of absorption by the D_2O stretching mode. These spectra have not been smoothed or deconvolved. The absorbance of both spectra were adjusted to zero only at 1800 cm^{-1}; the baselines return to zero in the vicinity of 1580 cm^{-1} without any other manipulations. Water vapor bands were not subtracted and account for some of the minor spectral features found at the same frequency in both polarizations.

Gramicidin in gramicidin/DMPC

The shape of the amide I absorption band for gramicidin is complex, and the signal-to-noise ratio does not justify attempts at self-deconvolution (Fig. 6). Nevertheless, this band must be resolved into analyzable components for the analysis of amide I transition moment order. For this purpose a bandfitting procedure was developed that borrows principles from "global analysis" routines, which have been widely applied in fluorescence lifetime analysis (Knutson et al., 1983; Axelsen et al., 1991). In this procedure, a set of spectra (typically several parallel and perpendicular pairs) are fit with a fixed number of bands. Each band is assigned an initial position, height, width, and shape (Gaussian versus Lorentzian). The procedure applies the simplex method (Press et al., 1986) to search for parameters providing the best fit to the experimental spectrum by a least-squares criterion. It differs from ordinary bandfit procedures in that multiple spectra are fit simultaneously, and the position, width, and shape of a given band are constrained to be identical for each spectrum in the set; only band height is allowed to vary between spectra.

This procedure was used to fit the amide I absorption of gramicidin with two symmetric bands, and it yields $R_z = 1.61 \pm 0.15$ for a component at 1658 cm^{-1}, and $R_z = 3.08 \pm 0.26$ for a component at 1634 cm^{-1} (results are from a simultaneous fit of five pairs of spectra ± SD; the fitting procedure yields bandwidths of 48 and 22 cm^{-1}, respectively, and a 99+% Gaussian band shape). We assume that the narrower, dominant, and highly anisotropic band at 1634 cm^{-1} arises from the carbonyl groups involved in intramolecular hydrogen bonds (see Discussion). The broader and rather isotropic band at 1658 cm^{-1} may well comprise multiple unresolved components. At this point, we have not yet developed a meaningful measure for the quality of this fit. The fit does seem to improve if we employ three or more bands, but then the procedure does not always converge to the same solution. Because we lack a firm theoretical basis for assigning specific frequencies to three or more bands, we did not give these results further consideration.

In Fig. 7 (*left*), the experimental result of $R_z = 3.08$ is used to calculate $\langle P_2(\cos\theta)\rangle$ for both $n_2 = 1.4$ and $n_2 = 1.5$ as a function of γ_ξ. In Fig. 7 (*right*), the NMR-derived gramicidin structure (provided to the authors by R. Ketchem and T. Cross, Florida State University, Tallahassee, FL) is used to calculate $\langle P_2(\cos\theta)\rangle$ as a function of α and θ. This figure shows that $\langle P_2(\cos\theta)\rangle$ has its maximum value of 0.78 when $\alpha = 0°$. $\langle P_2(\cos\theta)\rangle$ has its minimum possible value of 0.33 when $\gamma_\xi = 0°$ and $n_2 = 1.4$. These limiting values for $\langle P_2(\cos\theta)\rangle$ indicate that the angles θ and α are confined to the ranges 22–42° and 0–42°, respectively, and that the molecular order parameter for the gramicidin helix is >0.43.

The extreme values for each angle are highly unlikely in the case of gramicidin. One reason is that out-of-phase N—C stretching undoubtedly makes some contribution to amide I, so that α must be >0°. Another reason is that $\alpha = 42°$ implies $\gamma_\xi = 0°$, i.e., perfect molecular order and perfect

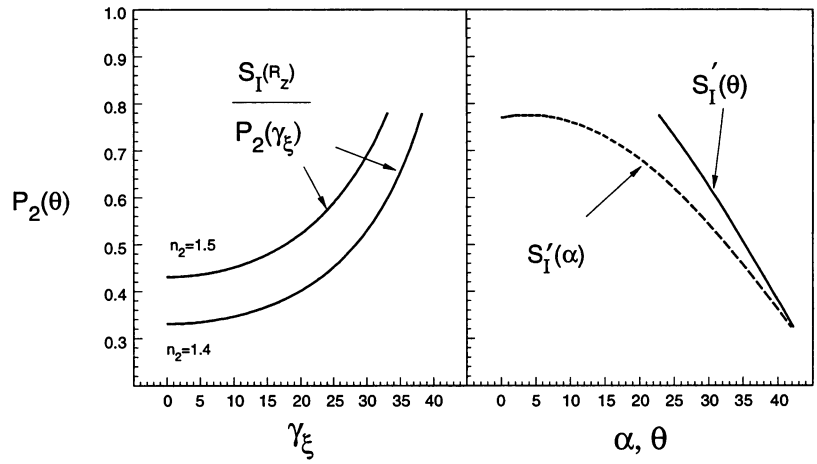

FIGURE 7 (*Left*) $P_2(\cos\theta)$ as a function of γ_ξ for the experimental result $R_z = 3.08$ from gramicidin. Plots for both $n_2 = 1.4$ and $n_2 = 1.5$ are shown. (*Right*) $\langle P_2(\cos\theta)\rangle$ as a function of α and θ for the NMR-derived structure of gramicidin. The curve labeled $S_I'(\alpha)$ is obtained directly from the equation given in Methods in which each value of α yields a set of n θ values. The curve labeled $S_I'(\theta)$ was obtained by equating $S_I'(\alpha) = P_2(\cos\theta)$ and solving for θ (see Appendix).

surface flatness. Considering the AFM and lipid order results given above, $\langle P_2(\cos)\ \gamma_\xi\rangle$ must be <1.0. This uncertainty notwithstanding, we conclude that PATIR-FTIR analysis of gramicidin in DMPC monolayers reveals a high degree of molecular order in both the peptide and lipid components of this experimental system, regardless of the value assigned to α.

DPPC in L_{24}/DPPC

L_{24} and acyl-deuterated DPPC were mixed at a 1:10 mol ratio in methanol. One drop of this solution was evaporated onto the end facet of our germanium ATR crystal in order to perform our studies under circumstances as similar as possible to those of Zhang et al. (1992a,b; 1995a,b,c).

The spectra shown in Fig. 8 result from a single internal reflection, and the bulk phase index is that of air ($n_3 = 1.0$). We estimate the number of lipid bilayers in this preparation by noting that the CD_2 symmetric stretching band in a monolayer study employing seven internal reflections exhibits an absorbance of ~2.3 mA at 2090 cm^{-1}. Thus an absorbance of 5 mA from a single reflection corresponds to approximately 15 monolayers or 7 to 8 bilayers. We employed acyl-deuterated DPPC to study the order of the lipid acyl chains without interference from CH_2 groups in the leucine side chains.

For CD_2 symmetric stretching at 2088.4 cm^{-1}, we find $R_z = 1.05$ (range 1.02–1.07, $n = 6$). Assuming that $\theta = 90°$, $n_2 = 1.45$, $n_3 = 1.0$ (air), and $P_2(\cos\xi) = 0.82$, we obtain $-2\,S_L(R_2)/\langle P_2(\cos\xi)\rangle = 0.60$. This is identical to our finding for DMPC above (despite major differences in sample preparation), and it supports the use of $P_2(\cos\xi) = 0.82$ as a "correction" factor in this sample. However, we are wary of applying this factor to lipid multilayers because it was derived for an acyl-silane surface and not for a lipid multilayer. We also looked at the CH_2 stretching absorption at 2850 cm^{-1} arising from side chains in the peptide and lipid headgroups. As expected, the order parameter derived from absorption at

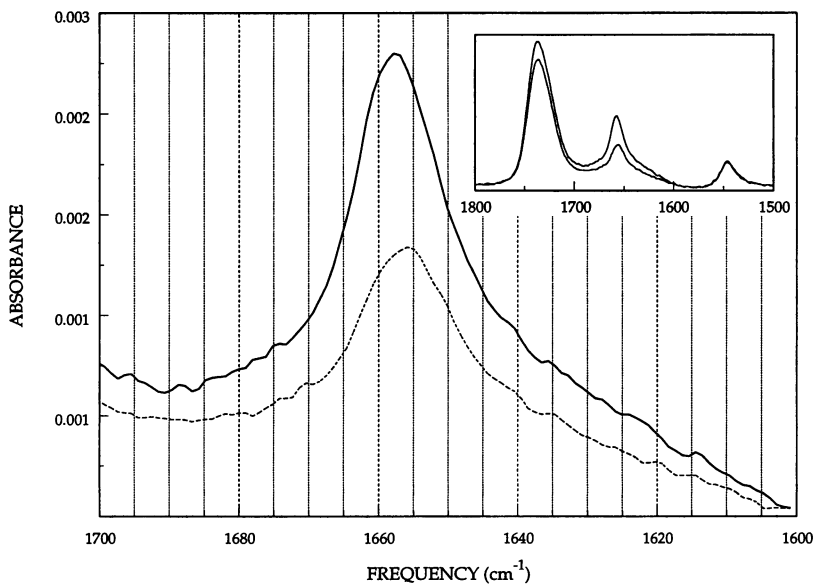

FIGURE 8 Parallel (*thick line*) and perpendicularly polarized (*thin line*) absorption spectra for a monolayer of acyl-deuterated DPPC and L_{24} in a 1:10 mol ratio. Inset: adjoining spectral regions showing baseline correction point (1800 cm^{-1}) and absorption due to lipid ester carbonyl stretching (1740 cm^{-1}). Samples of L_{24} were not subjected to H→D exchange, thus amide II is visible at 1545 cm^{-1}. The absorbance of both spectra were adjusted to zero only at 1800 cm^{-1}; the baselines return to zero in the vicinity of 1580 cm^{-1} without any other manipulations.

2850 cm^{-1} ranges from −0.17 to 0.02, suggesting very little order.

L_{24} in L_{24}/DPPC

The amide I absorption band of L_{24} (Fig. 8) exhibits a dichroic ratio of 2.09 (range 1.98–2.20, n = 6). As was done for gramicidin, we used this experimental result to calculate $\langle P_2(\cos\theta)\rangle$ for both n_2 = 1.4 and n_2 = 1.5 as a function of γ_ξ (Fig. 9, *left*). In Fig. 9 (*right*), model α-helices are used to determine $\langle P_2(\cos\theta)\rangle$ as a function of α and θ. This figure indicates that values of $\langle P_2(\cos\theta)\rangle$ are considerably higher for L_{24} than for gramicidin, with a maximum of 0.89 at $\alpha = 0°$ and a minimum of 0.52 when $\gamma_\xi = 0°$ and n_2 = 1.4. These limiting values for $\langle P_2(\cos\theta)\rangle$ imply that $\alpha < 20°$ and $\theta < 34°$ and that the molecular order $\langle P_2(\cos\gamma_\xi)\rangle$ for the L_{24} helix is >0.58.

In the case of L_{24}, dichroism measurements are also available for the amide II absorption band. We define θ_{II} analogously to that of θ for amide I (Fig. 2), except that the transition moment orientation relative to the peptide main chain differs. The inset of Fig. 8 indicates that R_z = 1.0 for amide II at 1545 cm^{-1}. $S_{II}(R_z)/\langle P_2(\cos\theta)\rangle$ is a minimum at $\theta_{II} = 90°$, so that for n_2 over the range of 1.4–1.5, the minimum value for $\langle P_2(\cos\gamma_\xi)\rangle$ ranges from 0.59 to 0.68. This result is comparable to that derived from the amide I absorption band. We also note that θ_{II} must be >68°; values lower than this imply a molecular order >1.0.

An important feature in the spectra of L_{24} (Fig. 8) is that the frequency maximum for the amide I absorption band in the perpendicular spectrum (1656.0 cm^{-1}) is 2.8 wavenumbers lower than that of the parallel spectrum (1658.8 cm^{-1}). Close inspection of the band shapes reveals some asymmetry, suggesting that they comprise multiple bands, but attempts to self-deconvolve these spectra did not yield clear component bands. This shift in position between these two polarizations most likely represents absorptions due to different symmetry species, namely types A and E_1, as predicted by normal mode calculations for α helices (Fanconi et al., 1969; Krimm and Bandekar, 1986; Krimm and Reisdorf, 1994). The implications of this finding are discussed below.

DISCUSSION

The determination of molecular order by PATIR-FTIR depends on accurate assumptions regarding optical parameters and angular relationships between the molecular axis and the amide I transition moment. In this work, we have examined and tested these assumptions by studying a nearly isotropic sample and two highly ordered peptides. We believe that the two peptides are well characterized as to their conformation and orientation in a lipid membrane and are faithfully applied to the germanium crystal surface under the conditions similar to those in which the characterizations have been performed. Our conclusions pertain to assumptions regarding instrumental parameters, gramicidin order, L_{24} order, and the influence of molecular symmetry on dichroic properties.

Parameters

It is difficult to find suitable reference samples for PATIR-FTIR studies. Requirements for an isotropic sample, for instance, are quite stringent. It must adsorb to the acylsilane coating of the germanium crystal from a dilute solution, but be insensitive to surface forces that may impart some anisotropy to the sample. Most compounds we tested either yielded evidence of ordered secondary structure or their absorption intensities changed over time. Among various globular proteins, hydrophobic peptides, amino acids, and semipolar compounds, NATA was the most suitable compound we found.

We used NATA to measure R_{ISO} in the vicinity of 1650–1630 cm^{-1}. R_{ISO} measurements are highly sensitive to the value of E_z^2, which is in turn inversely proportional to n_2^4. Although we cannot rule out a small degree of order for the amide I transition of NATA on our crystal surface, the degree of order suggested by the measurements is suffi-

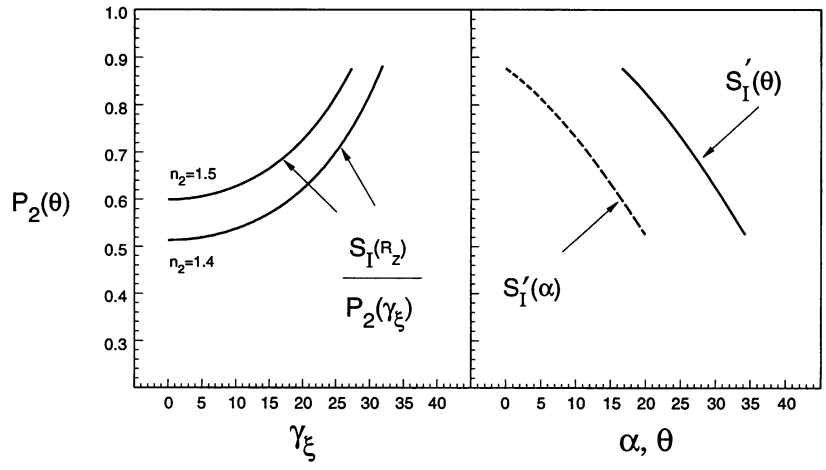

FIGURE 9 (*Left*) $P_2(\cos\theta)$ as a function of γ_ξ for the experimental result R_z = 2.09 from L_{24}. Plots for both n_2 = 1.4 and n_2 = 1.5 are shown. (*Right*) $P_2(\cos\theta)$ as a function of α and θ for α-helices excerpted from selected high resolution (<2.0 ANG) crystal structures and aligned with the z axis. Structures used (and residue numbers) include entries 1BTL (28–39, 74–85, 184–193, 203–212, 273–287), 1ECD (95–109), and 1GER (84–103, 313–325) from the Brookhaven Protein Data Bank. $S_I'(\alpha)$ and $S_I'(\theta)$ were derived as for Fig. 7.

ciently small that NATA helps to constrain the possible values of these crucial parameters, especially n_2. Values for n_2 must lie between 1.32 and 1.47 under the circumstances of our measurement, that is, for NATA adsorbed to an acyl-silane monolayer between 1650 and 1630 cm^{-1}. This range includes most of the values used in previous work by other investigators studying polypeptides in membranes, but it should be recognized that these values are estimates, not measured values. Despite being quoted with three digits of precision, they are largely untested aside from the results they yield, which seem reasonable. Until additional work definitively establishes the value of n_2 for supported lipid membranes, its value remains subject to some uncertainty.

Surface imperfections are not a consideration for measurements of R_{ISO} using NATA, but in principle they will limit the maximum possible order of an anisotropic sample. Our AFM measurements seem to place a limit of $\langle P_2(\cos \xi)\rangle i = 0.82$ on the contribution of surface imperfections to molecular disorder, and they suggest that local curvature on the surface is comparable to that of a 100-nm liposome. Progress has been made in preparing germanium crystal surfaces, which are flat on a scale of molecular dimensions (R. A. Dluhy, University of Georgia, personal communication, 1995), but at this point the technology required is prohibitively difficult to incorporate into our apparatus. Furthermore, eliminating surface imperfections will not yield more precise estimates for α or θ as long as γ remains unknown.

Gramicidin order

We have assumed that gramicidin adopts a $\beta^{6.3}$ conformation as described for a gramicidin dimer by the NMR studies of Arseniev et al. (1985) in detergent micelles, Prosser et al. (1991) in multilamellar DMPC dispersions, and Ketchem et al. (1993) in hydrated oriented DMPC multilayers. Dimeric and monomeric forms are in equilibrium in natural membranes, and therefore the $\beta^{6.3}$ conformation for the monomeric form is both plausible and probable under the circumstances of our measurements. It is unlikely that gramicidin adopts its bilayer-spanning double helix conformation because it is confined to a DMPC monolayer. Unfortunately, uncertainty in the appropriate values for α and θ leave this technique unable to positively distinguish between the double-helix form and the $\beta^{6.3}$-helix form using dichroism measurements.

Most of the amide I absorption of gramicidin is highly ordered and occurs at 1635 cm^{-1}. However, there is substantial absorption at 1650 cm^{-1}, which is not ordered. The latter is not surprising and most likely arises from carbonyl groups at either end of the gramicidin helix that are not involved in hydrogen bonds, or perhaps from ends of the helix which have "frayed." Denatured (presumably structureless) polypeptides absorb almost entirely at 1645–1650 cm^{-1} under these conditions (data not shown). Therefore, the appearance of highly dichroic absorption at 1635 cm^{-1} indicates that gramicidin has assumed considerable secondary structure in our experiments.

The shape of the amide I absorption band we obtain for gramicidin (Fig. 6) differs both from that reported for *N*-deuterated crystalline gramicidin by Naik and Krimm (1986a,b) and from those reported by Bouchard and Auger (1993) in thick DMPC multilayers prepared from various organic solvents. Our spectra are similar to those of Nabedryk et al. (1982) obtained in dried liposomes, although our numerical results differ in several respects, presumably because of their use of a dried liposome preparation, a dispersive-transmission instrument, and a $\pi^{4.4}$-helix model.

L_{24} order

Most (even very recent) PATIR-FTIR work involving α-helical peptides has relied on estimates of θ derived from transmission IR studies of polymeric aspartate or glutamate derivatives. These compounds were oriented by manually stroking organic solutions of these compounds as they dried to a thin film. Miyazawa and Blout (1961), for example, studied poly-γ-benzyl-L-glutamate and relied on the large frequency shift between the parallel and perpendicular components of amide II to determine that $\theta = 29–34°$ and $\theta_{II} = 75–77°$.

Superficially, our results indicating that $\theta < 34°$ and $\theta_{II} > 68°$ seem to be consistent with those of Miyazawa and Blout (1961), but closer inspection reveals a discrepancy. For example, if we use their value of $\theta_{II} = 76°$ for L_{24}, this implies (for $n_2 = 1.45$) that $P_2(\cos \gamma_\xi) = 0.78$. If this is true, then we see from Fig. 9 that our estimate for θ must be somewhat lower than theirs, i.e., 23–28°. Tsuboi (1962) studied the same compound as that of Miyazawa and Blout (1961) and employed related assumptions but concluded that $\theta = 39°$. Both of these studies showed amide I to lie at $\nu_{max} = 1650–1656$ cm^{-1}. Bradbury et al. (1962), on the other hand, studied poly-β-benzyl-L-aspartate and found $\nu_{max} = 1664$ cm^{-1}. Although this latter group concluded that $\theta = 33–41°$, they pointed out that their assumption about the "oriented fraction" of the polymer was "tenuous" and that the results of Miyazawa and Blout (1961) are suspect because they assumed that the polymer fiber axes were confined to the plane of the sample. Furthermore, a value of $\nu_{max} = 1664$ cm^{-1} indicates that the helices studied by Bradbury et al (1962) were most likely left-handed rather than right-handed (Bradbury et al, 1968). In summary, we cannot justify applying these values for θ, a priori, to the analysis of dichroism measurements made by PATIR-FTIR spectroscopy. This is especially true under circumstances in which ν_{max} for amide I differs because frequency shifts clearly imply that forces within a peptide have been altered.

Symmetry and dichroism

The foregoing treatment of α and θ in α-helices does not consider the implications of heterogeneous symmetry spe-

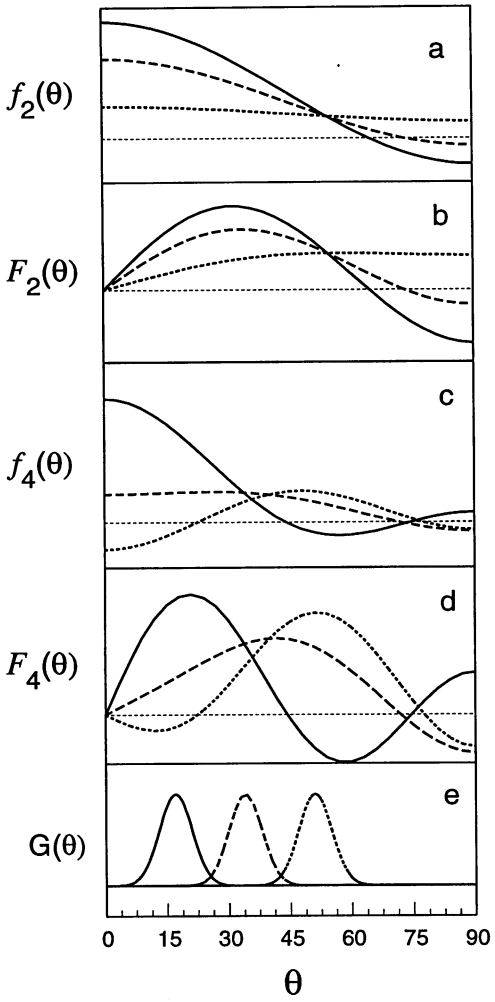

FIGURE 10 Comparative behavior of orientational and angular distribution functions using second- and fourth-order terms. In all panels, ——, - - - -, and · · · pertain to $\langle\theta\rangle$ = 17°, 34°, and 51°, respectively. (*a*) $f_2(\theta)$; (*b*) $F_2(\theta)$; (*c*) $f_4(\theta)$; (*d*) $F_4(\theta)$; and (*e*) Gaussian distributions with a half-width of 4°. The ordinate scales are arbitrary.

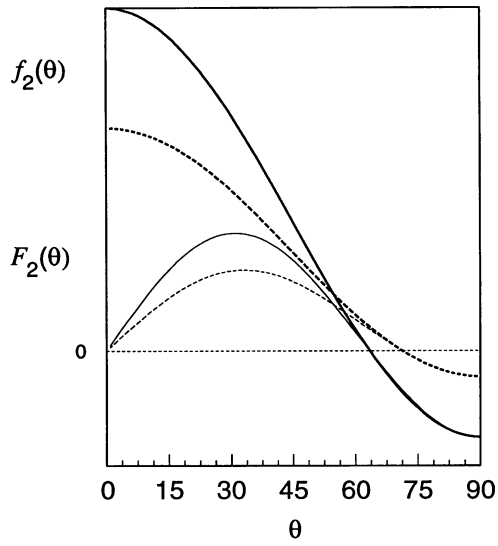

FIGURE 11 The comparative behavior of the second order distribution functions for $\langle P_2(\cos\gamma)\rangle$ = 0.58 (the minimum molecular order parameter possible for L_{24}, *dashed lines*), and $\langle P_2(\cos\gamma)\rangle$ = 1.00 (the maximum molecular order parameter possible, *solid lines*). The wide lines represent $f_2(\gamma)$, and the thin lines represent F_2.

cies absorbing in the amide I region. Normal mode analyses of α-helices suggest that two infrared-active vibrational modes absorb in the amide I region with differing symmetry properties and slightly different frequencies (Krimm and Bandekar, 1986). These differences have been observed in the helical polypeptides studied by Miyazawa and Blout (1961), Tsuboi (1962), and Bradbury et al. (1962) using transmission IR, but for reasons that are not yet clear, prior studies of α-helices that employ PATIR-FTIR techniques have not observed them (e.g., Smith et al., 1994).

The amide I mode designated type A is characterized by in-phase stretching of adjacent carbonyl groups. The mode designated type E_1 is actually a linear combination of two degenerate modes which are circularly polarized along the helix axis in opposite directions (Fanconi et al., 1969). The axial components of these modes cancel to yield a transition moment oriented perpendicular to the helix axis. It is important to note that this phenomenon will tend to decrease the measured R_z for a helix oriented perpendicular to the membrane surface and increase the apparent values for α and θ.

CONCLUSIONS AND SUMMARY

PATIR-FTIR studies of gramicidin and L_{24} indicate that both peptides form helices which preferentially orient perpendicular to the membrane surface. These conclusions are consistent with the structure and orientation expected for each compound and independent of assumptions about the orientation of the vibrational transition moments in the polypeptide main chain.

We have intentionally highlighted our uncertainty about the values of n_2, α, and θ in this work because the imprecision of values derived from older technologies is not often delineated. Indeed, some of the values derived from these older studies yield physically untenable results when applied to L_{24}. In one other instance in which this discrepancy has been noted, the sample involved was not a perfect α-helix, and this could conceivably explain the problem (Frey and Tamm, 1991). However, this is not the case with L_{24}, where the nature of its conformation is not at issue.

In the final analysis, it may be simplistic to seek a unique orientation for the amide I transition moment from infrared dichroism measurements if in fact there is more than one vibrational mode contributing to amide I. We must regard any values we derive as "apparent" or "effective" orientations for the transition moment and recognize that this value may vary as a sensitive function of polypeptide conformation and environment.

APPENDIX: The interpretation of $\langle P_2 \rangle$

In this work we assume that amide I transition moments are uniaxially distributed with respect to the surface normal. Under these conditions, the orientation distribution function, f, relates the probability of finding a transition moment at a specific orientation, to the angle between the transition moment and the surface normal, x, and is given in terms of Legendre polynomials by

$$f_m(x) = \frac{1}{2} \sum_n^m (2n + 1) \langle P_n(\cos x) \rangle P_n(\cos x)$$

for even $n \geq 0$ and order m. The corresponding angular distribution function, F, describes the probability of finding a transition moment at any given angle to the surface normal and is given by $F_m(x) = f_m(x) \sin x$. It should be noted that f is an incomplete description of the orientation distribution for finite values of m, and although

$$\int_0^\pi F_m(x)\, dx = 1$$

for all m, F is only approximate when f is incomplete.

These functions provide insight into the physical significance of $\langle P_2 \rangle$ when applied to a model α-helical peptide oriented perfectly perpendicular to the membrane surface (i.e., $\gamma = 0°$). In such a model, $\langle \theta \rangle$ is restricted to between 17 and 34° (see Fig.9), and its angular distribution is roughly Gaussian with a half-width of 4°. Given $P_0 = 1$, $\langle P_2 (\cos\theta) \rangle$ as defined above, and

$$\langle P_4(\cos \theta) \rangle = \tfrac{1}{8} \langle (35 \cos^4\theta - 30 \cos^2\theta + 3) \rangle$$

we compare $f_2(\theta)$, $F_2(\theta)$, $f_4(\theta)$, and $F_4(\theta)$ to Gaussian distributions of θ for $\langle \theta \rangle$ values of 17°, 34°, and 51° in Fig. 10.

Fig. 10 illustrates several interpretive difficulties we encounter when attempting to draw conclusions about these distribution functions using only information about $\langle P_2 \rangle$. First, for polynomials of order = 2, and $\langle \theta \rangle$ = 17–34°, the most probable orientation of the transition moment is $\theta = 0°$ (Fig. 10 *a*), and this cannot be true in an α-helix. Second, the angular distribution maximum for the second-order function does not correspond to $\langle \theta \rangle$ (Fig. 10 *b*), nor is it a sensitive function of $\langle \theta \rangle$ (Lafrance et al., 1993). When fourth-order terms are included, the most probable orientation may occur at angles other than zero, but only when $\langle \theta \rangle$ is >34° (e.g., 51°, Fig. 10 *c*). The fourth-order angular distribution does vary with $\langle \theta \rangle$ (Fig. 10 *d*), but ordinary absorption spectroscopy does not yield information from which terms of order ≥4 may be derived.

Third, $f_m(\theta)$ and $F_m(\theta)$ both assume negative values because of the truncation of order $>m$ terms. Clearly, functions truncated in this manner cease to be simple or physically intuitive probability functions. We may transform them into ordinary probability functions by employing additional assumptions regarding higher order terms (Deinum et al., 1988), but these assumptions are generally not valid if the molecular system possesses a collective tilt.

These difficulties must be confronted when employing relationships such as $\langle P_2(\cos \gamma + \theta) \rangle = \langle P_2(\cos \gamma) \rangle P_2(\cos \theta)$ on which several of the equations in the text depend. This relationship is valid as long as the transition moment is uniformly distributed around the molecular axis, and it permits $\langle P_2(\cos \gamma) \rangle$ from $\langle \theta \rangle$ and measurements of $\langle P_2 (\cos \gamma + \theta) \rangle$ to be derived. As just illustrated for $\langle P_2 (\cos \theta) \rangle$, however, the value of $\langle P_2(\cos \gamma) \rangle$ determines only the amplitude of an orientational distribution whose most probable value is $\gamma = 0°$. The molecular axes of a system may indeed be preferentially oriented at angles other than $\gamma = 0°$, but by itself we must conclude that $\langle P_2(\cos \gamma) \rangle$ is insufficient to determine the width of the angular distribution or to establish whether the molecular axis is preferentially tilted.

We illustrate this conclusion by plotting $f_2(\gamma)$ and $F_2(\gamma)$ for $\langle P_2(\cos \gamma_\xi) \rangle = 0.58$ (the minimum possible molecular order for L_{24}) and for $\langle P_2(\cos \gamma_\xi) \rangle = 1.00$ ("perfect" or maximal molecular order). As seen in Fig. 11, the plots of $f_2(\gamma)$ are similar in form, and plots of $F_2(\gamma)$ have maxima at the same angle. Clearly, one may not positively infer the presence of a collective molecular tilt from $\langle P_2(\cos \gamma_\xi) \rangle = 0.58$, but this value does imply a high degree of orientational order.

The authors wish to acknowledge S. Krimm, W. C. Reisdorf, R. Mendelsohn, and R. A. Dluhy for valuable dialogues; B. Roux, R. Ketchem, and T. Cross for molecular structure coordinates of gramicidin; and David Carroll for performing the AFM studies in the Laboratory for Research on the Structure of Matter at the University of Pennsylvania. P. H. Axelsen is supported by GM50805 and HL47469 from the National Institutes of Health and by a Biomedical Scholar Award from the L. P. Markey Charitable Trust. R. N. McElhaney is supported by an operating grant from the Medical Research Council of Canada and by major equipment grants from the Alberta Heritage Foundation for Medical Research.

REFERENCES

Arrondo, J. L. R., A. Muga, J. Castresana, and F. M. Goni. 1993. Quantitative studies of the structure of proteins in solution by Fourier-transform infrared spectroscopy. *Prog. Biophys. Mol. Biol.* 59:23–56.

Arseniev, A. S., I. L. Barsukov, V. F. Bystrov, A. L. Lomize, and Y. A. Ovchinnikov. 1985. ^{1}H-NMR study of gramicidin A transmembrane ion channel. *FEBS Lett.* 186:168–174.

Axelsen, P. H., Z. Bajzer, F. G. Prendergast, P. Cottam, and C. Ho. 1991. Resolution of fluorescence intensity decays of the two tryptophan residues in glutamine-binding protein of *E. coli* using tryptophan mutants. *Biophys. J.* 60:650–659.

Axelsen, P. H., W. D. Braddock, H. L. Brockman, C. M. Jones, R. A. Dluhy, B. S. Kaufman, and F. J. Puga. 1995. Use of internal reflectance infrared spectroscopy for the in situ study of supported lipid monolayers. *Appl. Spectrosc.* 49:526–531.

Bolen, E. J., and P. W. Holloway. 1990. Quenching of tryptophan fluorescence by brominated phospholipid. *Biochemistry.* 29:9638–9643.

Bradbury, E. M., L. Brown, A. R. Downie, A. Elliott, R. D. B. Fraser, and W. E. Hanby. 1962. The structure of the omega-form of poly-beta-benzyl-L-aspartate. *J. Mol. Biol.* 5:230–247.

Bradbury, E. M., B. G. Carpenter, and R. M. Stephens. 1968. Conformational studies of polymers and copolymers of L-aspartate esters. II. Infrared studies and the factors involved in the formation of the omega-helix. *Biopolymers.* 6:905–915.

Braiman, M. S., and K. J. Rothschild. 1988. Fourier-transform infrared techniques for probing membrane protein structure. *Annu. Rev. Biophys. Biophys. Chem.* 17:541–570.

Davis, J. H., D. M. Clare, R. S. Hodges, and M. Bloom. 1983. Interaction of a synthetic amphiphilic polypeptide and lipids in a bilayer structure. *Biochemistry.* 22:5298–5305.

Deinum, G., H. van Langen, G. van Ginkel, and Y. K. Levine. 1988. Molecular order and dynamics in planar lipid bilayers: Effects of unsaturation and sterols. *Biochemistry.* 27:852–860.

Fanconi, B., B. Tomilson, L. A. Nafie, W. Small, and W. L. Peticola. 1969. Polarized laser Raman studies of biological polymers. *J. Chem. Phys.* 51:3993–4003.

Fraser, R. D. B. 1953. The interpretation of infrared dichroism in fibrous protein structures. *J. Chem. Phys.* 21:1511–1515.

Fraser, R. D. B. 1956. Interpretation of infrared dichroism in fibrous proteins: the 2μ region. *J. Chem. Phys.* 24:89–95.

Fraser, R. D. B. 1958. Interpretation of infrared dichroism in axially oriented polymers. *J. Chem. Phys.* 28:1113–1115.

Fraser, R. D. B., and W. C. Price. 1952. Infrared dichroism and protein structure. *Nature.* 170:490–491.

Frey, S., and L. K. Tamm. 1991. Orientation of melittin in phospholipid bilayers. *Biophys. J.* 60:922–930.

Fringeli, U. P., Gunthard, H. H. 1981 Infrared membrane spectroscopy. *In* Membrane Spectroscopy. E. Grell, editor. Springer-Verlag, New York. 270–332.

Hansen, W. N. 1968. Electric fields produced by the propagation of plane coherent electromagnetic radiation in a stratified medium. *J. Opt. Soc. Am.* 58:380–390.

Hansen, W. N. 1972. Surface chemistry by reflection spectroscopy. *Prog. Nucl. Energy.* 11:3–35.

Hansen, W. N. 1973. Internal reflection spectroscopy in electrochemistry. *Adv. Electrochem. Electrochem. Eng.* 9:1–60.

Harrick, N. J. 1967 Internal Reflection Spectroscopy. Harrick Scientific Corporation, Ossining, New York.

Hulschilt, J. C., B. M. Millman, and J. H. Davis. 1989. Orientation of alpha-helical peptides in a lipid bilayer. *Biochim. Biophys. Acta.* 979: 139–141.

Ketchem, R. R., W. Hu, and T. A. Cross. 1993. High-resolution conformation of gramicidin A in a lipid bilayer by solid-state NMR. *Science.* 261:1457–1460.

Knutson, J. R., J. M. Beechem, and L. Brand. 1983. Simultaneous analysis of multiple fluorescence decay curves: a global approach. *Chem. Phys. Lett.* 102:501–507.

Krimm, S., and J. Bandekar. 1986. Vibrational spectroscopy and conformation of peptides, polypeptides, and proteins. *Adv. Protein Chem.* 38:181–364.

Krimm, S., and W. C. Reisdorf Jr. 1994. Understanding normal modes of proteins. *Faraday Discuss. Chem. Soc.* 96:1–17.

Lafrance, C.-P., P. Chabot, M. Pigeon, R. E. Prud'homme, and M. Pezolet. 1993. Study of the distribution of the molecular orientation in thick polyethylene samples by x-ray diffraction, infrared dichroism, and Raman spectroscopy. *Polymer.* 34:5029–5037.

Mantsch, H. H., and W. K.Surewicz. 1991 Probing protein secondary structure by infrared spectroscopy. *In* Proteins: Structure, Dynamics, and Design. V. Renugopalakrishnan, P. R. Carey, I. C. P. Smith, S. G. Huang, and A. C. Storer, editors. ESCOM, Leiden. 125–132.

Maoz, R., and J. Sagiv. 1984. On the formation and structure of self-assembling monolayers 1. A comparative ATR-Wettability study of Langmuir-Blodgett and adsorbed films on flat substrates and glass microbeads. *J. Colloid Interface Sci.* 100:465–496.

Miyazawa, T., and E. R. Blout. 1961. The infrared spectra of polypeptides in various conformations: Amide I and II bands. *J. Am. Chem. Soc.* 83:712–719.

Moser, M., D. Marsh, P. Meier, K. Wassmer, and G. Kothe. 1989. Chain configuration and flexibility gradient in phospholipid membranes: comparison between spin-label electron spin resonance and deuteron nuclear magnetic resonance, and identification of new conformations. *Biophys. J.* 55:111–123.

Myers, C. W., and S. L. Cooper. 1994. Analysis of some errors in the calculation of orientation functions for polymers from infrared dichroism measurements. *Appl. Spectrosc.* 48:72–77.

Nabedryk, E., M. P. Gingold, and J. Breton. 1982. Orientation of gramicidin A transmembrane channel: infrared dichroism study of gramicidin in vesicles. *Biophys. J.* 38:243–249.

Naik, V. M., and S. Krimm. 1986a. Vibrational analysis of the structure of gramicidin A. II. Vibrational spectra. *Biophys. J.* 49:1147–1154.

Naik, V. M., and S. Krimm. 1986b. Vibrational analysis of the structure of gramicidin A. I. Normal mode analysis. *Biophys. J.* 49:1131–1145.

Press, W. H., B. P. Flannery, S. A. Teukolsky, and W. T. Vetterling. 1986 Numerical Recipes. Cambridge University Press, Cambridge.

Prosser, R. S., and J. H. Davis. 1991. 2H Nuclear magnetic resonance of the gramicidin A backbone in a phospholipid bilayer. *Biochemistry.* 30:4687–4696.

Rice, D., and E. Oldfield. 1979. Deuterium nuclear magnetic resonance studies of the interaction between dimyristoylphosphatidylcholine and gramicidin A. *Biochemistry.* 18:3273–3279.

Rothschild, K. J., and N. A. Clark. 1979. Polarized infrared spectroscopy of oriented purple membrane. *Biophys. J.* 25:473–488.

Roux, B., and M. Karplus. 1994 Molecular dynamics simulations of the gramicidin channel. *In* Annual Review of Biophysics and Biomolecular Structure, 23rd ed. R. Stroud, C. Cantor, and T. Pollard, editors. Annual Reviews, Inc., Palo Alto. 731–761.

Sethna, P. P., K. F. Palmer, and D. Williams. 1978. Optical constants of D_2O in the infrared. *J. Opt. Soc. Am.* 68:815–817.

Smith, S. O., R. Jonas, M. Braiman, and B. J. Bormann. 1994. Structure and orientation of the transmembrane domain of glycophorin A in lipid bilayers. *Biochemistry.* 33:6334–6341.

Susi, H., S. N. Timasheff, and L. Stevens. 1967. Infrared spectra and protein conformations in aqueous solutions I. The amide I band in H_2O and D_2O solutions. *J. Biol. Chem.* 242:5460–5466.

Tsuboi, M. 1962. Infrared dichroism and molecular conformation of alpha-form poly-γ-benzyl-L-glutamate. *J. Poly. Sci.* 59:139–153.

Wallace, B. A. 1992. Crystallographic studies of a transmembrane ion channel, gramicidin A. *Prog. Biophys. Mol. Biol.* 57:59–69.

Zhang, Y. P., R. N. A. H. Lewis, R. S. Hodges, and R. N. McElhaney. 1992a. FTIR spectroscopic studies of the conformation and amide hydrogen exchange of a peptide model of the hydrophobic transmembrane alpha-helices of membrane proteins. *Biochemistry.* 31:11572–11578.

Zhang, Y. P., R. N. A. H. Lewis, R. S. Hodges, and R. N. McElhaney. 1992b. Interaction of a peptide model of a hydrophobic transmembrane alpha-helical segment of a membrane protein with phosphatidylcholine bilayers: differential scanning calorimetric and FTIR spectroscopic studies. *Biochemistry.* 31:11579–11588.

Zhang, Y. P., R. N. A. H. Lewis, R. S. Hodges, and R. N. McElhaney. 1995a. Interaction of a peptide model of a hydrophobic transmembrane alpha-helical segment of a membrane-protein with phosphatidylethanolamine bilayers: differential scanning calorimetric and Fourier-transform infrared spectroscopic studies. *Biophys. J.* 68:847–857.

Zhang, Y. P., R. N. A. H. Lewis, G. D. Henry, B. D. Sykes, R. S. Hodges, and R. N. McElhaney. 1995b. Peptide models of helical hydrophobic transmembrane segments of membrane-proteins: 1. studies of the conformation, intrabilayer orientation, and amide hydrogen exchangeability of Ac-K_2-$(LA)_{12}$-K_2-amide. *Biochemistry.* 34:2348–2361.

Zhang, Y. P., R. N. A. H. Lewis, R. S. Hodges, and R. N. McElhaney. 1995c. Peptide models of helical hydrophobic transmembrane segments of membrane-proteins: 2. differential scanning calorimetric and FTIR spectroscopic studies of the interaction of Ac-K_2-$(LA)_{12}$-K_2-amide with phosphatidylcholine bilayers. *Biochemistry.* 34:2362–2371.